Thiol−Disulfide Exchange in an Immunoglobulin-like Fold: Structure of the N-Terminal Domain of DsbD[†,‡]

Celia W. Goulding,[§] Michael R. Sawaya,[§] Angineh Parseghian,[§] Vincent Lim,[||] David Eisenberg,[§] and Dominique Missiakas*[,||]

Howard Hughes Medical Institute and Laboratory of Structural Biology and Molecular Medicine, UCLA-DOE, P.O. Box 951570, Los Angeles, California 90095-1570, and Department of Biochemistry and Molecular Biology, The University of Chicago, 920 East 58th Street, Chicago, Illinois 60637

Received December 13, 2001; Revised Manuscript Received March 22, 2002

ABSTRACT: *Escherichia coli* DsbD transports electrons across the plasma membrane, a pathway that leads to the reduction of protein disulfide bonds. Three secreted thioredoxin-like factors, DsbC, DsbE, and DsbG, reduce protein disulfide bonds whereby an active site C-X-X-C motif is oxidized to generate a disulfide bond. DsbD catalyzes the reduction of the disulfide of DsbC, DsbE, and DsbG but not of the thioredoxin-like oxidant DsbA. The reduction of DsbC, DsbE, and DsbG occurs by transport of electrons from cytoplasmic thioredoxin to the C-terminal thioredoxin-like domain of DsbD ($DsbD^C$). The N-terminal domain of DsbD, $DsbD^N$, acts as a versatile adaptor in electron transport and is capable of forming disulfides with oxidized DsbC, DsbE, or DsbG as well as with reduced $DsbD^C$. Isolated $DsbD^N$ is functional in electron transport in vitro. Crystallized $DsbD^N$ assumes an immunoglobulin-like fold that encompasses two active site cysteines, C_{103} and C_{109}, forming a disulfide bond between β-strands. The disulfide of $DsbD^N$ is shielded from the environment and capped by a phenylalanine (F_{70}). A model is discussed whereby the immunoglobulin fold of $DsbD^N$ may provide for the discriminating interaction with thioredoxin-like factors, thereby triggering movement of the phenylalanine cap followed by disulfide rearrangement.

Folding of secreted proteins within the periplasm of *Escherichia coli* requires the formation of disulfide bonds, a process that is dependent on the Dsb[1] (*d*isulfide *b*ond) proteins. Disulfide bond formation occurs via oxidation of a pair of cysteine sulfhydryl groups, a reaction that is catalyzed by DsbA. Electrons generated by oxidative folding are transferred from DsbA to DsbB and channeled into the electron transport chain (*1*, *2*) (Figure 1a). DsbA cannot provide a proofreading activity for improperly formed disulfides which are repaired by DsbC, DsbD, DsbE, and DsbG. For example, maturation of *c*-type cytochromes requires first oxidation and then reduction of two cysteine residues. The reduction of cystines within *c*-type cytochromes is catalyzed by DsbE (*3*, *4*). Such redox rearrangement of the apocytochromes is needed to prevent random oxidation of the cysteines that are involved in the covalent attachment of heme. Reshuffling of incorrectly paired disulfide bonds of periplasmic proteins is also initiated by a reduction reaction that involves DsbC or DsbG (*5*, *6*). In all of these reactions, DsbC, DsbG, and DsbE act as electron donors. As no source of reducing equivalent is generated in the bacterial periplasm, Gram-negative cells have evolved a pathway whereby DsbD transfers electrons from cytoplasmic NADPH across the cytoplasmic membrane to DsbC, DsbE, and DsbG (Figure 1a) (*7*, *8*).

DsbC, DsbG, and DsbE exist in reduced [Dsb-$(SH)_2$] and oxidized [Dsb-S_2] states. Only reduced Dsb-$(SH)_2$ can transfer electrons to target substrates. In these redox-active proteins, two sulfhydryl groups, $-(SH)_2$, are positioned in a dithiol C-X-X-C motif. This motif was first characterized for thioredoxin, a small ubiquitous cytoplasmic protein that reduces disulfide bonds in the cytoplasm (*9*, *10*). The crystal structures of both DsbC (*11*) and DsbE (*12*) reveal the presence of a thioredoxin-like domain bearing the redox active C-X-X-C motif. DsbG shares sequence similarity with DsbC and is therefore presumed to contain a thioredoxin fold. Furthermore, the C-terminal domain of DsbD, $DsbD^C$ (residues 450−546), resembles protein disulfide isomerase, another member of the thioredoxin superfamily. Both the N- and C-terminal domains of DsbD, $DsbD^N$, and $DsbD^C$, respectively, are located in the periplasm (*13*, *14*), and each harbors a pair of cysteines, $C_{103}-C_{109}$ and $C_{461}-C_{464}$, respectively (Figure 1b). $DsbD^N$ and $DsbD^C$ are connected by eight transmembrane (TM) segments with three cysteine residues. Five out of the seven cysteines of DsbD are absolutely required for electron transport activity (C_{103}, C_{109}, C_{163}, C_{285}, and C_{461}) (*13*). C_{163} and C_{285} are located in TM1 and TM4, respectively (Figure 1b).

Previous work examined the mechanism whereby DsbD transfers electrons from the cytoplasm to the periplasm. Electron transfer mediated by DsbD was demonstrated by

[†] This work was supported by Department of Energy Grant DOE ER 60615-1004936-0000034 to D.E. and by U.S. Public Health Service Grants GM62410 and GM58266 to D.E. and D.M., respectively.

[‡] The coordinates for $DsbD^N$ have been deposited in the Brookhaven Protein Data Bank with the accession number 1L6P.

* To whom correspondence should be addressed: dmissiak@bsd.uchicago.edu.

[§] UCLA-DOE.

[||] The University of Chicago.

[1] Abbreviations: Dsb, disulfide bond formation; TrxA, thioredoxin; TrxB, thioredoxin reductase; $DsbD^N$, the N-terminal domain of DsbD (1−144 amino acids); $DsbD^C$, the C-terminal thioredoxin-like domain of DsbD.

10.1021/bi016038l CCC: $22.00
Published on Web 05/09/2002

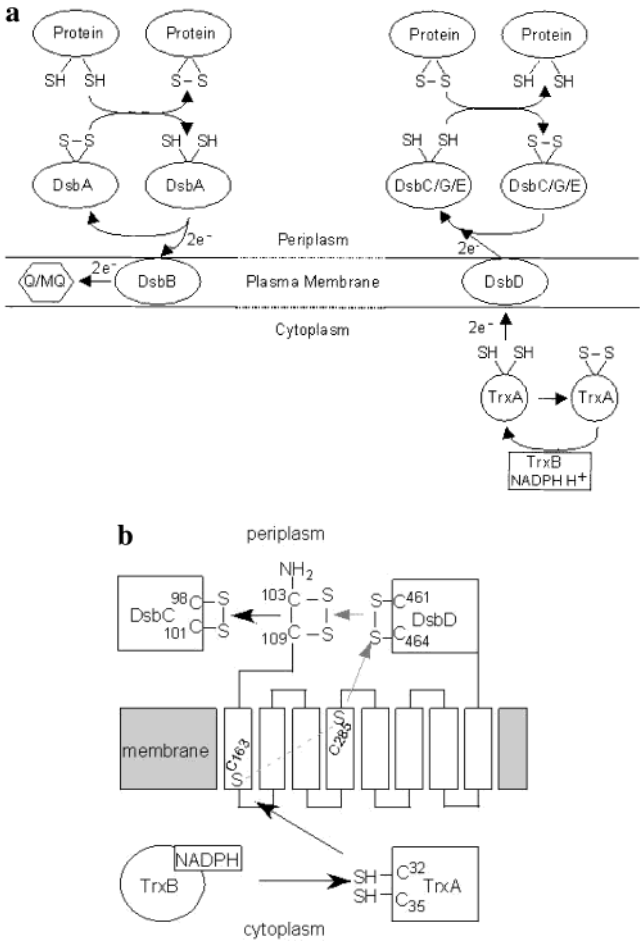

FIGURE 1: Model for disulfide bond formation and rearrangement catalyzed by Dsb proteins of *E. coli*. (a) Known Dsb proteins in the *E. coli* system. DsbA oxidizes disulfide bonds of newly translocated proteins. The transmembrane protein DsbB accepts electrons from DsbA and transfers them to quinone or menaquinones embedded in the bilayer. DsbC and DsbG are disulfide isomerase proteins that catalyze the re-formation of incorrectly formed disulfide bonds. DsbE is thought to reduce the cysteines of aopcytochrome *c* for heme attachment (anchoring of DsbE in the plasma membrane is not depicted on the figure). These three proteins accept electrons from the cytoplasm through the DsbD transmembrane protein. (b) Model for DsbD-mediated transfer of electrons across the cytoplasmic membrane. TrxB (NADPH) donates electrons to the active site dithiol motif of TrxA, C_{32}-X-X-C_{35}. C_{32} of TrxA interacts with C_{163} of DsbD. This presumably resolves the disulfide between C_{163} and C_{285} of DsbD (represented as a gray broken line). In the next step, C_{163} and C_{285} presumably donate electrons to the dithiols at C_{461} and C_{464}. The reduced dithiol of C_{461} attacks the disulfide at C_{103} and C_{109}, which transfer electrons to the oxidized dithiol motif of DsbC. The square-shaped box indicates the presence of a thioredoxin-like fold. Dark arrows indicate the steps supported by experimental data whereas gray arrows indicate steps presumed to occur.

isolating reaction intermediates that are tethered by a disulfide bond between redox-active proteins (*15*). Such extremely short-lived intermediates can be captured using redox proteins containing only half of the redox-active site. Substitution of DsbD C_{285} with alanine and TrxA C_{35} with serine (C_{32}-G-P-S_{35}) led to the production of a stable complex. Characterization of this complex showed that the two proteins are trapped in a mixed disulfide species with a disulfide bond between C_{32} of TrxA and C_{163} of DsbD, suggesting that TrxA resolves a disulfide between C_{163} and C_{285} of DsbD. Upon TrxA-mediated reduction, C_{285} must transfer electrons to C_{461} and C_{464} of DsbD, as substitution of C_{461} in the C-terminal thioredoxin-like domain of DsbD (C_{461}-V-A-C) with alanine abolishes electron transfer. The C-terminal domain is assumed to transfer electrons to the N-terminal domain of DsbD, presumably by forming a disulfide between C_{109} and C_{461}. Electron transfer also involves a reduction of the DsbC dithiol motif (C_{98}-G-Y-C) and occurs between DsbC and $DsbD^N$. Coexpression of DsbD C_{103}A and DsbC C_{101}A, but not of DsbC C_{98}A or DsbD C_{109}A, leads to the formation of a mixed disulfide species between the two Dsb proteins. Thus, the final step of DsbD-mediated electron transfer likely occurs via thiol−disulfide exchange between C_{109} of DsbD and C_{98} of DsbC (*16*).

All electron transfer steps examined for DsbD occur by a specific mechanism, i.e., the intramolecular exchange of thiol−disulfide bonds (*15*, *17*). Thioredoxin (TrxA) transfers electrons to the transmembrane domain of DsbD. Electrons are transferred to $DsbD^C$ but not to DsbA, DsbC, DsbE, or DsbG, even though all of these proteins contain a thioredoxin-like fold. Specificity may be solely achieved by proximity of the two domains and the intramolecular nature of the reaction. Electrons are then transferred to $DsbD^N$. $DsbD^N$ selectively transfers electrons to DsbC, DsbE, and DsbG but not to DsbA or DsbB (*16*). $DsbD^N$ functions as an adaptor unit that permits electron transfer between thioredoxin moieties but avoids futile electron cycling between reductants such as DsbC or DsbG and the oxidant DsbA. Nonetheless, $DsbD^N$ itself must possess redox qualities of thioredoxins as its sulfhydryls must be able to receive and donate electrons very rapidly. We have crystallized $DsbD^N$ and describe structural features that likely contribute to the remarkable redox properties of the active site cysteines.

MATERIALS AND METHODS

Protein Purification. The nucleotide sequence encoding $DsbD^N$ was amplified by the polymerase chain reaction using the following 5′- and 3′-primers: gtttttgccggtccttcgacgcgccg and aagaattcacaattgcgcggtgggctg, respectively. The fragment was cloned in vector pGEX-2T (Pharmacia) using the restriction sites *Bam*HI and *Eco*RI. The protein was expressed as a glutathione *S*-transferase N-terminal DsbD (GST-$DsbD^N$) fusion protein in *E. coli* using DH5α cells. Ten milligrams of protein was obtained from an 8 Lculture induced at an OD_{600nm} of 0.2 with 1 mM IPTG for 3 h at 37 °C. Cells were collected by centrifugation, suspended in 50 mM Tris-HCl, pH 7.5, 150 mM NaCl, and 10% glycerol, and broken in a French press. $DsbD^N$ was recovered with the total soluble proteins by ultracentrifugation for 1 h at 100000*g*. This soluble fraction was loaded on a glutathione−Sepharose column (Pharmacia), and washed with 10 volumes of buffer. $DsbD^N$ was cleaved from bound GST by thrombin digestion as described by the manufacturer (Pharmacia). Cleaved $DsbD^N$ was further purified over mono-Q−Sepharose using 20 mM Tris-HCl, pH 6.4, and eluted with a gradient of NaCl from 0 to 250 mM. $DsbD^N$ eluted at 30−50 mM NaCl. Mass spectrometry analysis of $DsbD^N$ revealed a mass of 16073, which corresponds to the expected mass for the 144 amino acid protein domain (16072.78). As predicted from the cloning procedure, the $DsbD^N$ sequence initiates with the expected Gly followed by Ser instead of Leu.

Crystallization and Structure Determination. Initial crystallization of purified $DsbD^N$ was carried out by concentrating

Table 1: X-ray Diffraction Data Collection and Atomic Refinement for *E. coli* $DsbD^N$ [a]

	iodide	native
data		
wavelength (Å)	1.5418	1.5418
resolution range (Å)	90−2.3	100−1.65
unique reflections (total)[b]	1981 (19542)	18609 (155538)
completeness (%)	99.4 (97.4)	98.5 (96.5)
R_{merge}[c]	10.0 (50.4)	7.4 (38.2)
$I/\sigma(I)$	22.7 (3.47)	28.2 (5.11)
no. of *I* sites/monomer	11	
phasing resolution range (Å)	48.2−1.65	
figure of merit[d]	0.405/0.651	
model refinement		
resolution range (Å)	10−1.65	
no. of reflections (working/free)	17500/783	
no. of protein atoms	958	
no. of water molecules	290	
R_{cryst}/R_{free}[e] (%)	13.9/21.5	
rms deviations		
bond lengths (Å)	0.009	
bond angles (deg)	1.137	

[a] The second column refers to the iodide derivative, and the third column refers to the native protein. [b] Statistics for the highest resolution shell are given in parentheses. [c] $R_{merge}(I) = \sum_{hkl}[(\sum_i|I_{hkl,j} - \langle I_{hkl}\rangle|)/\sum_i I_{hkl,i}]$. [d] Values are given before density modification at 2.5 Å and after density modification and phase extension to 1.65 Å resolution. [e] $R_{cryst} = \sum_{hkl}||F_o| - |F_c||/\sum_{hkl}|F_o|$. R_{free} was computed identically, except that 5% of the reflections were omitted as a test set.

the protein to 10 mg/mL using 0.1 M Tris-HCl, and 0.5 M NaCl, pH 7.4. The protein crystallized in 25% poly(ethylene glycol) 4000, 0.1 M sodium acetate, pH 4.6, and 0.2 M NH_4-SO_4. The crystals were swiped through a solution of 20% glycerol and crystallization buffer (1:1) before mounting and collecting data under cryoconditions. Potassium iodide soaks were performed with 0.5 M potassium iodide in the cryoprotectant. The crystals were soaked for 1 min before mounting under cryoconditions. An iodo derivative of the $DsbD^N$ crystal diffracted to 2.3 Å, and a native crystal diffracted to 1.65 Å with cell dimensions of 53.21 × 55.63 × 102.05 Å with one monomer per asymmetric unit in space group $C222_1$. Data were processed using DENZO and SCALEPACK (*18*). SIRAS phasing proceeded by the usual methods of heavy atom location [SHELXD (http://shelx.uni-ac.gwdg.de/SHELXD/)], maximum likelihood phase refinement [ML-PHARE (*19*)], and density modification [DM (*20*)]. Phase extension to 1.65 Å permitted automated model building with ARP/wARP (*21*) of all of the residues of $DsbD^N$ except the initial 3 residues (1−3) and the last 21 residues (124−144). Model building was done in O (*22*), and the model was refined using SHELXL. Data and refinement statistics are presented in Table 1.

Structure and Sequence Analysis. BLAST (*23*) and CLUSTALW (*24*) were used for database searches and multiple sequence alignments, respectively. Pairwise alignments were calculated using the Smith−Waterman algorithm. Similar protein structures were searched using DALI (*25*) and aligned with combinatorial extension (CE) (*26*). Figure 2b is illustrated using SETOR (*27*).

RESULTS

Members of the thioredoxin superfamily display small amounts of sequence similarity and are predicted to assume similar three-dimensional folded structures. An active site C-X-X-C motif undergoes reversible oxidation−reduction and is present in all members of the thioredoxin superfamily. The primary sequence of $DsbD^N$ does not display sequence similarity with thioredoxin, and $DsbD^N$ is not predicted to assume a thioredoxin-like fold. Further, $DsbD^N$ does not harbor the characteristic C-X-X-C motif. Comparison of several different DsbD-like proteins revealed the presence of a Q-G-C_{103}-X_5-C_{109}-Y sequence motif within $DsbD^N$ (Figure 2a), where C_{109} is implicated in the redox reaction that transfers electrons from DsbD to DsbC (*15*). Purified, recombinant $DsbD^N$ was able to transfer electrons and hence reduced oxidized DsbG in vitro (data not shown). When used in substoichiometric amounts over DsbG, $DsbD^N$ could still reduce oxidized DsbG provided stoichiometric amounts of the purified and reduced C-terminal domain of DsbD, $DsbD^C$, were added to the reaction mixture (data not shown). Together, these data suggested that $DsbD^N$ is a functional domain, as it is capable of accepting electrons from $DsbD^C$ and transferring them to DsbG.

Overall Structure of $DsbD^N$. $DsbD^N$ is a single domain that consists of four antiparallel sheets, two of which form a β-sandwich (Figure 2b). The initial 3 residues (1−3) and the last 21 residues (124−144) are presumably disordered. The β-sandwich consists of two larger antiparallel β-sheets, each of which has three strands (β1, β2, β8 and β4, β10, β12, respectively). On one edge of the β-sandwich is an elongated segment of seven residues (residues 57−63, between β5 and β6) and two β-sheets, one near the N-terminus and the other near the C-terminus of $DsbD^N$. The residues of the elongated segment have the backbone torsion angles consistent with a β-strand. Nonetheless, this elongated segment is not hydrogen bonded to the neighboring β-strand (β5); instead, the hydrophobic side chains point into the core of the protein. At the N-terminal end of $DsbD^N$, the five-stranded antiparallel β-sheet is reminiscent of a partial β-barrel (β6, β7, β3, β10, β11). At the C-terminal end is another short antiparallel β-sheet which consists of three β-strands (β5, β9, β13). The only helical secondary structure is a four-residue α-helix (α1) located at the beginning of β-strand 1, which lies against the five-stranded β-sheet (Figure 2b). The Ramachandran plot shows that all residues except two, Q_{26} and D_{79}, are in the allowed region. The model locates residues Q_{26} and D_{79} in a β-turn, which fits the electron density map extremely well.

Structural Features of the Active Site. Noticeably, the structure of $DsbD^N$ displays two striking features. First, the two cysteines, C_{103} and C_{109}, which have been shown to be essential for activity, form a disulfide bond between strand β10 and strand β11 (Figure 2b). The distance between the two Sγ atoms of C_{103} and C_{109} is 2.05 ± 0.05 Å, which is consistent with a disulfide bond linking the two residues (normally 2.030 Å) (*28*). The closest side-chain atoms to the disulfide bond are the aromatic ring carbons of F_{70} (3.34 Å); OH of Y_{42} (3.55 Å) and OH of Y_{40} (4.37 Å); O of D_{68} (5.07 Å); NH_2 of Q_{101} (5.12 Å); and Y_{71} (6.19 Å) (Figure 2c). With the exceptions of F_{70} and Y_{71}, which appear to be interchangeable in position, all of these residues are conserved among homologues of $DsbD^N$ as shown by the sequence alignment in Figure 2a. Another region of conserved residues is found in the first α-helix (α1) near the active site, where the aromatic ring of F_{18} is pointing toward the active site contributing to its surrounding hydrophobic

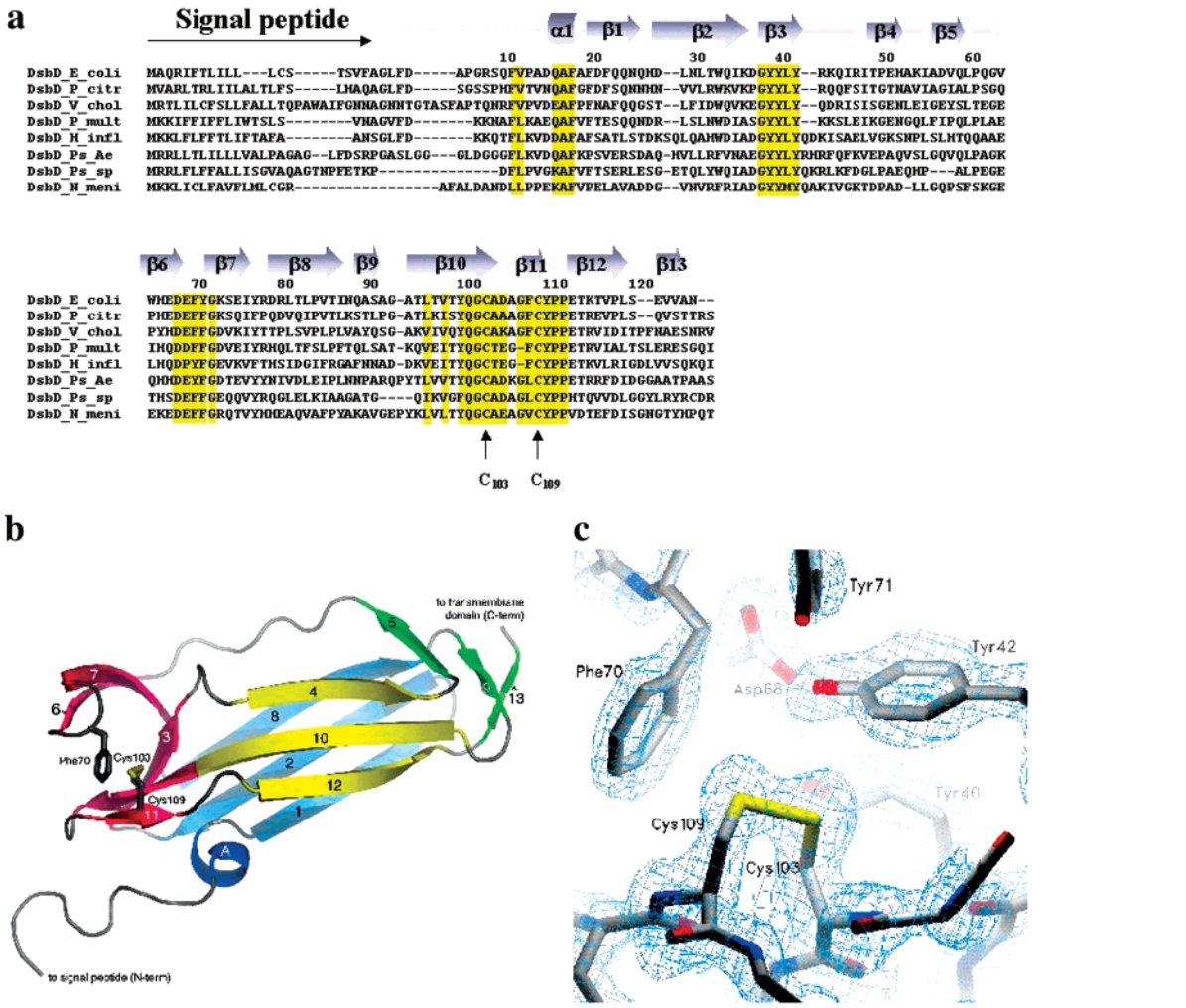

FIGURE 2: Structure of *E. coli* DsbD^N. (a) Sequence comparison of DsbD^N homologues. The top diagram depicts the *E. coli* DsbD^N protein in terms of secondary structure elements (residue numbering is for the *E. coli* mature sequence). The yellow boxes show conserved residues among the sequences. The two active site cysteines are indicated with arrows. The sequence alignment was made with CLUSTALW and BoxShade. (b) Ribbon diagram of DsbD^N. DsbD^N contains four β-sheets and one α-helix, A. The β-sheets contributing to the immunoglobulin-like β-sandwich are colored in yellow and blue. The active site is located on the partial β-barrel (red); the sulfur atoms of the disulfide bond (C_{103} and C_{109}) are in yellow, the atoms of the aromatic ring of F_{70} capping C_{109} are shown in white, and all β-carbon atoms are shown in white. The β-sheet located at the C-terminal end of the protein appears in green. This figure was generated using SETOR. (c) The active site of DsbD^N as a view of the final $2F_o - F_c$ electron density map. The electron density (blue) is contoured at 1.5σ. The distance between the two sulfur atoms (yellow) in the disulfide bond form is 2.05 ± 0.05 Å. The figure shows the residues surrounding the active site (Y_{40}, Y_{42}, D_{68}, F_{70}, and Y_{71}) with oxygen atoms shown in red, nitrogen atoms in blue, and carbon atoms in white. The figure was generated using Pymol.

environment. Notably, nearly all of the conserved residues are located in or around the active site.

The second striking feature is the loop region between strands β6 and β7, which lies over the disulfide bond between C_{103} and C_{109} of the active site. Both β6 and β7 strands are located on the five-stranded β-sheet (appearing in red in Figure 2b). These residues are also in a conserved region of the protein (Figure 2a). In particular, the aromatic ring of F_{70} within this loop region is situated approximately 160° across from the disulfide bond within this partial β-barrel. F_{70} forms an aromatic−sulfur interaction with the Sγ atom of C_{109} with a 62° angle and may contribute to the stability of the disulfide bond. This loop lies over the otherwise exposed active site cysteine residues. As C_{109} is "capped" by F_{70}, we think it is plausible that the loop protects the active site from illegitimate redox reactions and refer to this region as the "cap" of DsbD^N. Our model implies that structural displacement of the cap from the active site must occur prior to reduction of the disulfide bond of DsbD^N by DsbD^C. Further, electron transfer between DsbD^N and its protein substrates DsbC, DsbG, and DsbE may also involve a mechanism that requires cap displacement. Overall, the disulfide bond is stabilized by S−π interactions via four aromatic rings from residues F_{70}, Y_{40}, Y_{42}, and Y_{71}, and C_{103} has a strong hydrophobic interaction with Y_{42} (*29*).

The N- and C-termini of DsbD^N are located at the opposite ends of the elongated domain. This is not unexpected as the N-terminal is the cleavage site for the signal peptide, and the C-terminal disordered strand is anchored to the hydrophobic transmembrane core of DsbD. It is noteworthy that the electrostatic molecular surface potential at the C-terminal end of DsbD^N is hydrophobic, whereas the surface around the active site five-stranded partial β-barrel is negatively charged with arginine side chains protruding at the surface.

Structurally Related Proteins. A search for structurally related proteins in the Brookhaven Protein Data Bank,

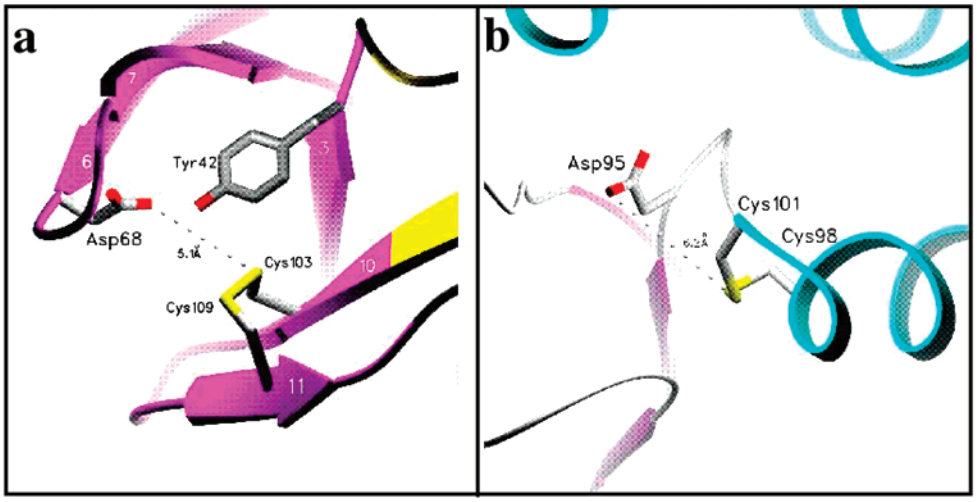

FIGURE 3: Structure of DsbC and DsbD^N active sites. (a) Structure of the DsbD^N active site in the partial β-barrel (pink). The distance between D_{68} and C_{103} is 5.1 Å; the hydroxyl group of Y_{42} is positioned between these two residues. (b) Structure of the DsbC active site. C_{98} and C_{101} are disulfide bonded, bridging the α-helix (cyan) and the loop shown in white. An aspartic residue, D_{95}, is found 6.2 Å away from C_{101}. The sulfurs atoms are shown in yellow, oxygen atoms in red, nitrogen atoms in blue, and carbon atoms in white. Both active sites are illustrated in SETOR.

performed with the DALI server, identified proteins that are involved in cell membrane-adhesion and membrane-interacting proteins. The closest structural homologue of DsbD^N was found to be the ap-2 clathrin adaptor α subunit with a *Z*-score of 7.1 (*30*). Also, there are structural similarities to invasin, immunoglobulins, and major histocompatibility proteins. The fold of DsbD^N is part of the immunoglobulin superfamily. This family of fold is normally comprised of a single β-sandwich, whereas DsbD^N contains two additional antiparallel β-sheets. The structural homology search gave no positive results for proteins that function as a thiol−disulfide oxidoreductant, as does DsbD^N.

DISCUSSION

Proteins with similar function often share evolutionary relationships that can be revealed by similarities in their tertiary structures. Redox reactions involving reversible thiol−disulfide exchanges are often carried out by dithiols arranged in a C-X-X-C motif within a thioredoxin-like fold. Three of the Dsb proteins have been shown to have thioredoxin folds, including *E. coli* DsbA (*31*), DsbC (*11*), and the DsbE homologue from *Mycobacterium tuberculosis* (*12*). Sequence homology (24% identity) suggests that the structure of DsbG is similar to that of DsbC. Presumably, the C-terminal domain of DsbD also adopts a thioredoxin-like fold. Conversely, some thioredoxin-like domains do not carry any redox activity. Protein disulfide isomerase contains four thioredoxin folds, of which two are redox inactive with no C-X-X-C motif (*32*). In *E. coli* and other organisms, thioredoxin is maintained reduced by thioredoxin reductase (TrxB). TrxB is not a member of the thioredoxin superfamily. Electrons are transferred from the C_{135} and C_{138} of TrxB to thioredoxin (*33*). Recycling (reduction) of C_{135} and C_{138} is achieved intramolecularly by an accessory domain that uses flavin adenine dinucleotide as a cofactor. Much like TrxB, DsbD^N does not belong to the thioredoxin superfamily. DsbD^N obtains reducing equivalent intramolecularly from a thioredoxin-like domain (DsbD^C) and in turn reduces three thioredoxin-like proteins. To our knowledge, the redox activity of DsbD^N is the first of its kind for an immunoglobulin-like fold.

As for thioredoxin, DsbD^N-mediated thiol−disulfide oxidoreduction is achieved by formation of mixed disulfide intermediates between the first cysteine of thioredoxin-like domains and C_{109} of DsbD^N. C_{109}, the active thiolate and its redox partner, C_{103}, are located on two separate, short, antiparallel β-strands (Figure 3a). How does the active site of thioredoxin-like proteins compare with that of DsbD^N? Active site thiolates of thioredoxin-like proteins are stabilized by electrostatic interactions with local positively charged residues and presumably by an α-helix "dipole" (*34*−*36*). In the thioredoxin fold, the C-X-X-C motif is always located at the N-terminus of the α-helix dipole, and the second cysteine is the third amino acid of the α-helix (Figure 3b). The first thiol has an unusually low pK_a value, and it has been suggested that the electrostatic field associated with the α-helix pointing with its N-terminus toward the cysteine residue is in part responsible for lowering the thiol pK_a value by up to 5 pH units in glutaredoxin and DsbA (*35*, *36*). In thioredoxin, the thiolate form of C_{32}, which is essential for the nucleophilic attack, is stabilized by an interaction with the thiol hydrogen of C_{35}. The preference for deprotonating C_{32} before C_{35} arises in part because of the greater solvent exposure of C_{32}, due to its location before the α-helix (*34*). Other reports have concluded that redox properties of the thioredoxin-like protein, i.e., propensity to contain a thiolate at the active site, may be influenced by the two amino acids (X-X) surrounded by the two cysteines in the active site (C-X-X-C) (*37*, *38*). Obviously, the contribution of the helix dipole does not account for the thiolate form of C_{109} of DsbD^N. However, a close look at the active site suggests that, in DsbD^N, C_{109} thiolate is stabilized by a hydrogen-bonding network and electrostatic interactions strikingly reminiscent of those of thioredoxins (Figures 2c and 3). Numerous residues surrounding C_{103} and C_{109} in the structure are conserved among DsbD homologues. These highly conserved amino acids are boxed in yellow in Figure 2a. Assuming that, as for thioredoxins, the structure of reduced

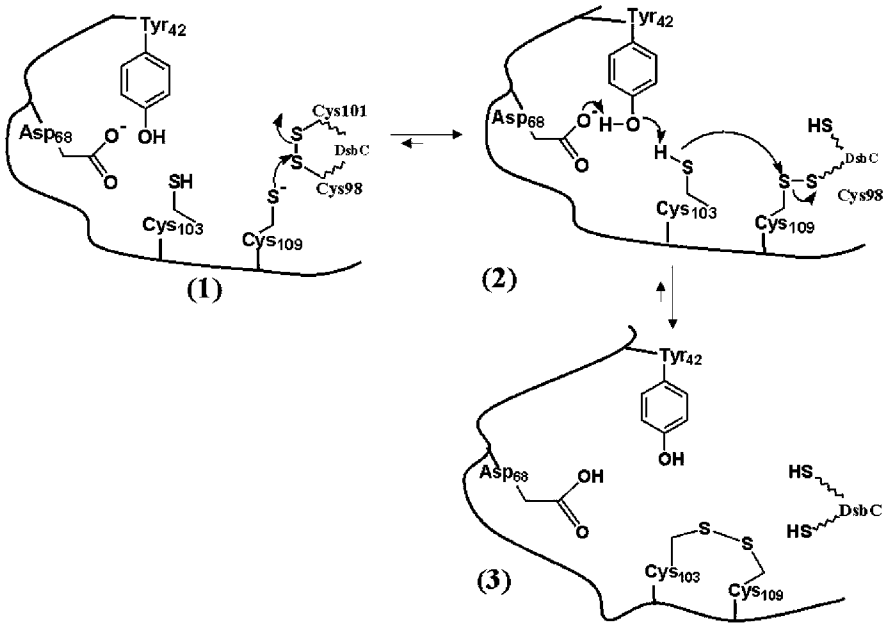

FIGURE 4: Reduction mediated by $DsbD^N$: a possible mechanism. (1) The thiolate form of the solvent-accessible C_{109} performs a nucleophilic attack on the oxidized target protein, DsbC, leading to an intermolecular disulfide bond between C_{109} of $DsbD^N$ and C_{98} of DsbC. (2) Proton transfer between C_{103} and D_{68} is mediated by the hydroxyl group of Y_{42} and triggers the nucleophilic attack of C_{103} on the mixed disulfide bridge. (3) Release of reduced DsbC and oxidized $DsbD^N$.

$DsbD^N$ is similar to that of oxidized $DsbD^N$, the closest side-chain atoms to the cysteines will be the hydroxyl groups of Y_{42} (3.55 Å), Y_{40} (4.37 Å), and Y_{71} (5.32 Å) (Figure 2c). The oxygen and hydroxyl group of D_{68} lie at 5.42 Å from the sulfhydryl of C_{109}. D_{68} is conserved in all but one amino acid sequence of DsbD homologues (Figure 2a). Helix α1 near the active site is also composed of conserved amino acids. The conserved sequence $E_{69}FYGK_{73}$, between strand β4 and β5, appears as a loop capping the active site cysteines C_{103} and C_{109}, and the aromatic ring of F_{70} lies directly over C_{109} of the disulfide bond (2.48 Å). This capping appears to protect the disulfide bond, which would be otherwise solvent exposed and susceptible to nucleophilic attack (Figure 2b).

$DsbD^N$ receives electrons from $DsbD^C$ and reduces oxidized DsbC, DsbE, and DsbG. $DsbD^C$, DsbC, DsbE, and DsbG must all displace the "$E_{69}FYGK_{73}$" cap, allowing for preferential deprotonation of C_{109} over C_{103} which remains buried. The thiolate form of C_{109} performs a nucleophilic attack on oxidized DsbC, leading to an intermolecular disulfide bridge (Figure 4, step 1) (*15*, *17*). We propose that this event is followed by proton transfer between C_{103} and the conserved D_{68} and subsequent nucleophilic attack on the mixed disulfide bridge (Figure 4, step 2). This is followed by release of reduced DsbC and oxidized $DsbD^N$ (Figure 4, step 3). This model is reinforced by studies using thioredoxin showing that a conserved aspartic residue (D_{26}) serves as a proton transfer catalyst for thioredoxin's C_{35} thiol during the formation and breakdown of mixed disulfide intermediates (*39*). A water molecule may possibly mediate proton transfer between D_{26} and C_{35} (*40*). The distance between these two residues is 6 Å (*41*), which is very close to the 5.1 Å measured between the carboxyl group of D_{68} and the sulfur atom of C_{103} in $DsbD^N$ (Figure 3a). Further, we propose that in $DsbD^N$ proton transfer between D_{68} and C_{103} is mediated by the hydroxyl group of Y_{42}, instead of a water molecule. The distance between the sulfur atom of C_{103} and the hydroxyl group of Y_{42} is 3.51 Å, and it is 2.69 Å between the hydroxyl group of Y_{42} and the carboxyl group of D_{68} (Figure 3a). We note that a conserved aspartic residue, D_{95}, can also be observed in the structure of DsbC (*11*), in the vicinity of the buried C_{101} (Figure 3b). The side chains of these two residues are separated by 6.2 Å. In the reduced form of $DsbD^N$, C_{103} and Y_{42} must move slightly nearer, allowing proton transfer to occur between the three residues (Figure 4, step 2). Also, the hydrophobic environment of the active site disulfide bond will enhance the transfer of electrons and protons within the partial β-barrel. This suggested catalytic diad between D_{68} and Y_{42} is reminiscent of the well-known catalytic triad of serine, histidine, and aspartic acid found in serine proteases. Δ^5-3-Ketosteroid isomerase is another enzyme containing similar residues in the catalytic site (three tyrosines, two aspartates) (*42*).

How does $DsbD^N$ select it substrates as compared to DsbC or DsbA? DsbC shares structural features with DsbA, including a helical insert in the thioredoxin fold. This helical insert is smaller in the case of DsbC, and it is not clear what its role might be (*11*). Both DsbA and DsbC contain a cleft to accommodate potential substrates. The architecture of these clefts is very different. The DsbA cleft is thought to bind substrate peptide (*31*) and is absent in DsbC. Unlike DsbA, DsbC is a homodimer with a much larger, uncharged broad cleft, lying at the interface of the homodimer (*11*). It has been hypothesized that this uncharged cleft permits binding of unfolded proteins. Loose binding of unfolded polypeptides may allow the proteins to experience various conformations for the correct disulfide bonds to form. It is unclear from our data whether $DsbD^N$ interacts with DsbC in a similar manner. However, it is possible that the cap region of $DsbD^N$ may contact this region of DsbC during catalysis, as would a nonfolded substrate.

In $DsbD^N$, electron transfer between thioredoxin folds is mediated by an unrelated fold closely related to the immunoglobulin fold. The cysteines in this immunoglobulin-like fold are less promiscuous than those in the thioredoxin fold,

as no mixed disulfides have been observed between $DsbD^N$ and random proteins containing dithiol−disulfide groups (*15*). Immunoglobulin-like folds are not uncommon in the periplasm of *E. coli*. PapD, a chaperone involved in assembly of PapK pilin subunits, contains an immunoglobulin fold (*43*). The crystal structure of the PapD−PapK chaperone−subunit complex revealed that the chaperone functions by donating one β-strand to complete the immunoglobulin-like fold of the subunit, via a mechanism termed donor strand exchange (*44*). This stable interaction prevents premature oligomerization of a pilus subunit such as PapK, until export at the PapC outer membrane protein export site. However, since interactions between $DsbD^N$ and its redox partners are transient, it is unlikely that strand exchange is required to bring the two folds together.

In another immunoglobulin-like fold, that of the chaperone Caf1M from *Yersinia pestis*, oxidation of two cysteine residues is thought to activate the chaperone activity of Caf1M (*43*, *45*, *46*). Oxidation is mediated by DsbA (*46*, *47*) on two cysteines located on two successive β-strands, as predicted from the structure of PapD. Caf1M is a periplasmic chaperone involved in the assembly of composite adhesive pili. Thus, this is an example of a protein predicted to have an immunglobulin-like fold (Caf1M) that interacts with a thioredoxin-like protein (DsbA) to become active. Unlike $DsbD^N$, however, Caf1M is not itself redox active, as it does not oxidize any substrates subsequently.

Clearly, the $DsbD^N$ immunoglobulin-like fold is a variation of a common fold that has developed a relatively new electron-transporting function, perhaps uniquely tailored to provide reducing equivalents for thiol−disulfide exchanges coupled to protein folding in bacterial cells. In a pathway of interacting thioredoxin-like partners, $DsbD^N$ is shown to adopt a completely different three-dimensional structure; nonetheless, it carries a very similar function and strikingly an almost identical catalytic site. This is likely an instance of convergent evolution where two proteins evolved independently, quite like the bacterial protease subtilisin and trypsin proteases which have a very similar geometry of residues in their active site but no structural similarities (*48*, *49*). The structure of $DsbD^N$ and its proposed mechanism will allow for careful probing of the residues that catalyze reduction and oxidation of the active site cysteines.

ACKNOWLEDGMENT

We thank K. Faull for mass spectrometry measurements, D. Cascio for invaluable help with data collection and general crystallography, M. Gingery, G. Kleiger, C. Mura, and M. Apostol for discussion, and O. Schneewind for carefully reading the manuscript.

REFERENCES

1. Kobayashi, T., Kishigami, S., Sone, M., Inokuchi, H., Mogi, T., and Ito, K. (1997) *Proc. Natl. Acad. Sci. U.S.A. 94*, 11857−11862.
2. Bader, M., Muse, W., Ballou, D. P., Gassner, C., and Bardwell, J. C. (1999) *Cell 98*, 217−227.
3. Thony-Meyer, L. (2000) *Biochim. Biophys. Acta 1459*, 316−324.
4. Raina, S., and Missiakas, D. (1997) *Annu. Rev. Microbiol. 51*, 179−202.
5. Zapun, A., Missiakas, D., Raina, S., and Creighton, T. E. (1995) *Biochemistry 34*, 5075−5089.
6. Bessette, P. H., Cotto, J. J., Gilbert, H. F., and Georgiou, G. (1999) *J. Biol. Chem. 274*, 7784−7792.
7. Missiakas, D., Schwager, F., and Raina, S. (1995) *EMBO J. 14*, 3415−3424.
8. Rietsch, A., Bessette, P., Georgiou, G., and Beckwith, J. (1997) *J. Bacteriol. 179*, 6602−6608.
9. Russel, M. (1995) *Methods Enzymol. 252*, 264−274.
10. Holmgren, A. (1995) *Structure 3*, 239−243.
11. McCarthy, A. A., Haebel, P. W., Torronen, A., Rybin, V., Baker, E. N., and Metcalf, P. (2000) *Nat. Struct. Biol. 7*, 196−199.
12. Goulding, C. W., Parseghian, A., Gennaro, M., and Eisenberg, D. (2002) (manuscript in preparation).
13. Chung, J., Chen, T., and Missiakas, D. (2000) *Mol. Microbiol. 35*, 1099−1109.
14. Gordon, E. H., Page, M. D., Willis, A. C., and Ferguson, S. J. (2000) *Mol. Microbiol. 35*, 1360−1374.
15. Krupp, R., Chan, C., and Missiakas, D. (2001) *J. Biol. Chem. 276*, 3696−3701.
16. Bader, M. W., Hiniker, A., Regeimbal, J., Goldstone, D., Haebel, P. W., Riemer, J., Metcalf, P., and Bardwell, J. C. (2001) *EMBO J. 20*, 1555−1562.
17. Katzen, F., and Beckwith, J. (2000) *Cell 103*, 769−779.
18. Otwinowski, Z. M. W. (1997) *Methods Enzymol. 276A*.
19. Project, C. C. (1994) *Acta Crystallogr. D 50*, 760−763.
20. Cowtan, K., and Main, P. (1998) *Acta Crystallogr. D 54*, 487−489.
21. Perrakis, A., Morris, R., and Lamzin, V. S. (1999) *Nat. Struct. Biol. 6*, 458−463.
22. Jones, T. A., Zou, J. Y., Cowan, S. W., and Kjeldgaard, M. (1991) *Acta Crystallogr. A 47*, 110−119.
23. Altschul, S. F., Boguski, M. S., Gish, W., and Wootton, J. C. (1994) *Nat. Genet. 6*, 119−129.
24. Thompson, J. D., Higgins, D. G., and Gibson, T. J. (1994) *Nucleic Acids Res. 22*, 4673−4680.
25. Holm, L., and Sander, C. (1993) *J. Mol. Biol. 233*, 123−138.
26. Shindyalov, I. N., and Bourne, P. E. (1998) *Protein Eng. 11*, 739−747.
27. Evans, S. V. (1993) *J. Mol. Graphics 11*, 134−138.
28. Engh, R. A., and a. H., R. (1991) *Acta Crystallogr. A 47*, 392−400.
29. Reid, K. S. C., Lindley, P. F., and Thornton, J. M. (1985) *FEBS Lett. 190*, 209−213.
30. Traub, L. M., Downs, M. A., Westrich, J. L., and Fremont, D. H. (1999) *Biochemistry 96*, 8907−8912.
31. Martin, J. L., Bardwell, J. C., and Kuriyan, J. (1993) *Nature 365*, 464−468.
32. Kemmink, J., Darby, N. J., Dijkstra, K., Nilges, M., and Creighton, T. E. (1997) *Curr. Biol. 7*, 239−245.
33. Lennon, B. W., Williams, C. H. J., and Ludwig, M. L. (2000) *Science 289*, 1190−1194.
34. Dillet, V., Dyson, H. J., and Bashford, D. (1998) *Biochemistry 37*, 10298−10306.
35. Guddat, L. W., Bardwell, J. C., and Martin, J. L. (1998) *Structure 6*, 757−767.
36. Schirra, H. J., Renner, C., Czisch, M.,., Huber-Wunderlich, M., Holak, T. A., and Glockshuber, R. (1998) *Biochemistry 37*, 6263−6276.
37. Mossner, E., Huber-Wunderlich, M., Rietsch, A., Beckwith, J., Glockshuber, R., and Aslund, F. (1999) *J. Biol. Chem. 274*, 25254−25259.
38. Grauschopf, U., Winther, J. R., Korber, P., Zander, T., Dallinger, P., and Bardwell, J. C. (1995) *Cell 83*, 947−955.
39. LeMaster, D. M., Springer, P. A., and Unkefer, C. J. (1997) *J. Biol. Chem. 272*, 29998−30001.
40. Menchise, V., Corbier, C., Didierjean, C., Saviano, M., Benedetti, E., Jacquot, J.-P., and Aubrey, A. (2001) *Biochem. J. 359*, 65−75.
41. Dyson, H. J., Jeng, M. F., Tennant, L. L., Slaby, I., Lindell, M., Cui, D. S., Kuprin, S., and Holmgren, A. (1997) *Biochemistry 36*, 2622−2636.
42. Kim, S. W., Cha, S.-S., Cho, H.-S., Ha, N.-C., Cho, M.-J., Joo, S., Kim, K. K., Choi, K. Y., and Oh, B.-H. (1997) *Biochemistry 36*, 14030−14036.

43. Holmgren, A., and Branden, C. I. (1989) *Nature 342*, 248−251.
44. Sauer, F. G., Futterer, K., Pinkner, J. S., Dodson, K. W., Hultgren, S. J., and Waksman, G. (1999) *Science 285*, 1058−1061.
45. MacIntyre, S., Zyrianova, I. M., Chernovskaya, T. V., Leonard, M., Rudenko, E. G., Zav'Yalov, V. P., and Chapman, D. A. (2001) *Mol. Microbiol. 39*, 12−25.
46. Zav'yalov, V. P., Chernovskaya, T. V., Chapman, D. A., Karlyshev, A. V., MacIntyre, S., Zavialov, A. V., Vasiliev, A. M., Denesyuk, A. I., Zav'yalova, G. A., Dudich, I. V., Korpela, T., and Abramov, V. M. (1997) *Biochem. J. 324*, 571−578.
47. Jacob-Dubuisson, F., Pinkner, J., Xu, Z., Striker, R., Padmanhaban, A., and Hultgren, S. J. (1994) *Proc. Natl. Acad. Sci. U.S.A. 91*, 11552−11556.
48. Phadtare, S., Rao, M., and Deshpande, V. (1996) *Arch. Microbiol. 166*, 414−417.
49. Liao, D. I., and Remington, S. J. (1990) *J. Biol. Chem. 265*, 6528−6531.

BI016038L